Available online at www.sciencedirect.com
SCIENCE DIRECT
Surface & Coatings Technology 200 (2006) 5717–5724
SURFACE & COATINGS TECHNOLOGY
www.elsevier.com/locate/surfcoat

Corrosion behavior of magnetron sputtered α-Ta coatings on smooth and rough steel substrates

Sung Min Maeng [a,*], Lisa Axe [a], Trevor A. Tyson [b], Leszek Gladczuk [c], Marek Sosnowski [c]

[a] Department of Civil and Environmental Engineering, New Jersey Institute of Technology, Newark, NJ 07102, USA
[b] Department of Physics, New Jersey Institute of Technology, Newark 07102, USA
[c] Department of Electrical and Computer Engineering, New Jersey Institute of Technology, Newark 07102, USA

Received 28 October 2004; accepted in revised form 15 August 2005
Available online 13 October 2005

Abstract

α-Ta coatings on smooth and rough steel substrates (AISI 4340) were studied in an effort to assess the resulting porosity and corrosion behavior. While the long-range crystallographic orientation of the coatings was found to be affected by the surface roughness, the short-range structure was invariant. Peak broadening in X-ray diffraction patterns attributed to microstrain and particle size was observed for coatings on both types of substrates as compared to Ta powder. Although the roughness was two orders of magnitude greater for the coatings deposited on the rough substrates than the smooth ones, the porosity was not significantly different. Furthermore, electrochemical impedance behavior over long exposure times of coatings deposited on smooth and rough steel substrates was similar to that of Ta foil. These results demonstrate that substrate roughness appears to have little to no effect on the coating quality with respect to corrosion performance for 50 μm coatings.

Keywords: Tantalum; Magnetron sputtering; Substrate roughness; Electrochemical impedance spectroscopy; X-ray absorption spectroscopy; Corrosion behavior

1. Introduction

Tantalum hard coatings deposited by physical vapor deposition (PVD) have been investigated to protect gun-bore from erosion and corrosion as bulk Ta (α phase) exhibits excellent physical and chemical properties such as a high melting point (2996 °C), good ductility, and excellent corrosion resistance in aggressive environments [1,2]. However, when deposited as a film on steel substrates, either the α-phase (body-centered cubic structure), β-phase (tetragonal structure), or a mixture of both phases has been observed under varying deposition conditions [3,4]. Since β-Ta is brittle, α-phase is preferred in protecting gun-bore against erosion. Additionally, the β phase has been reported to be more susceptible to delamination than the α-phase and hence to be less corrosion resistant [5].

Coating qualities such as density, thickness, and porosity are important in corrosion resistance [6–8]. Our previous study investigating corrosion behavior as a function of thickness showed that α-Ta coatings, 50 μm or more in thickness, behaved as well as Ta foil [5]. In this earlier work, the steel substrate was polished down to the r.m.s. roughness of 50 nm using a diamond suspension. Surface preparation of substrates can critically affect the morphology of PVD deposits. In particular, substrate surface roughness have been shown to influence the corrosion behavior [9], as an increased substrate roughness resulted in more coating defects due to a shadowing effect during PVD film growth. A study on the relationship between surface roughness and pinhole formation in TiN films showed that a smoother substrate surface yielded a lower pinhole density, resulting in improved corrosion resistance [10]. As the peak-to-valley height on the substrate profile increases, there is an increasing tendency for coating defects to form. Liu et al. [11] studied the coating porosity of a PVD CrN on mild steel substrates prepared by grinding with 220 grit SiC and polishing with 6 and 45 μm diamond paste. They observed a reduction in coating defects with decreasing surface roughness. While our earlier work demonstrated that viable corrosion resistant α-Ta coatings with a thickness of 50 μm or greater

* Corresponding author. Tel.: +1 973 596 6077; fax: +1 973 596 5790.
E-mail address: smm8166@njit.edu (S.M. Maeng).

0257-8972/$ - see front matter © 2005 Elsevier B.V. All rights reserved.
doi:10.1016/j.surfcoat.2005.08.128

were produced on polished AISI 4340 steel substrates, the objective of this study is to compare the corrosion behavior of the coatings deposited on smooth and rough surfaces, the latter of which may be more representative of the actual gun-bore condition.

2. Experimental details

AISI 4340 steel coupons (1.26×1.26 cm^2) were prepared by grinding with 60 grit aluminum oxide for the rough surface simulating potentially the gun-bore, and by mechanical polishing with a diamond suspension down to 0.05 μm for the smooth surface. Both types of substrates were then cleaned electrochemically and in an ultrasonic bath of organic solvents (acetone, followed by alcohol). After loading into the sputtering chamber, the substrates were baked in vacuum at 200 °C by an internal halogen lamp for at least 6 h. Prior to deposition, the substrates were sputter-etched for 10 min with Ar at a pressure of 30 Pa and a DC bias of −400 V. The α-Ta coatings of 50 μm (±20%) thickness were deposited by DC magnetron sputtering in argon gas (99.995% purity) at a pressure of 0.7 Pa [4,5]. The base pressure in the process chamber was 1.1×10^{-5} Pa. A tantalum target (99.95%) with a 50 mm diameter was mounted 50 mm below the substrate holder. The initial deposition rate was 1.2 nm/s, up to 3 μm thickness, and then the source current was increased to 1 A with a target voltage of −375 V, resulting in a deposition rate of 2.4 nm/s. The substrates were at the ground potential. Without intentional substrate heating, depositions produced β-Ta coatings. Temperature of the substrate during deposition was held at approximately 420 °C, using a substrate heater. Details of the apparatus and the deposition procedure are given elsewhere [4].

Ta foil (99.9%) and the rough and polished steel substrates (AISI 4340) were used as reference samples in electrochemical tests.

Characterization included crystallographic phase identification with X-ray diffraction (XRD) and microscopic roughness measurements with atomic force microscopy (AFM). Before and after the corrosion tests, the surface and corrosion features of coated samples were examined using a field emission scanning electron microscope (FE-SEM) with qualitative elemental analysis by energy dispersive X-ray spectroscopy (EDX). Additionally, to obtain local structural information, extended X-ray absorption spectroscopy (EXAFS) experiments using total electron yield (TEY) mode were carried out at the Ta L_{III} edge (E_0=9881 eV) on beamline X11A at the National Synchrotron Light Source (NSLS), Brookhaven National Laboratory. The storage ring operated at the energy of 2.80 GeV with an average current of 180 mA. A Si (111) double-crystal monochromator was used for the photon energy

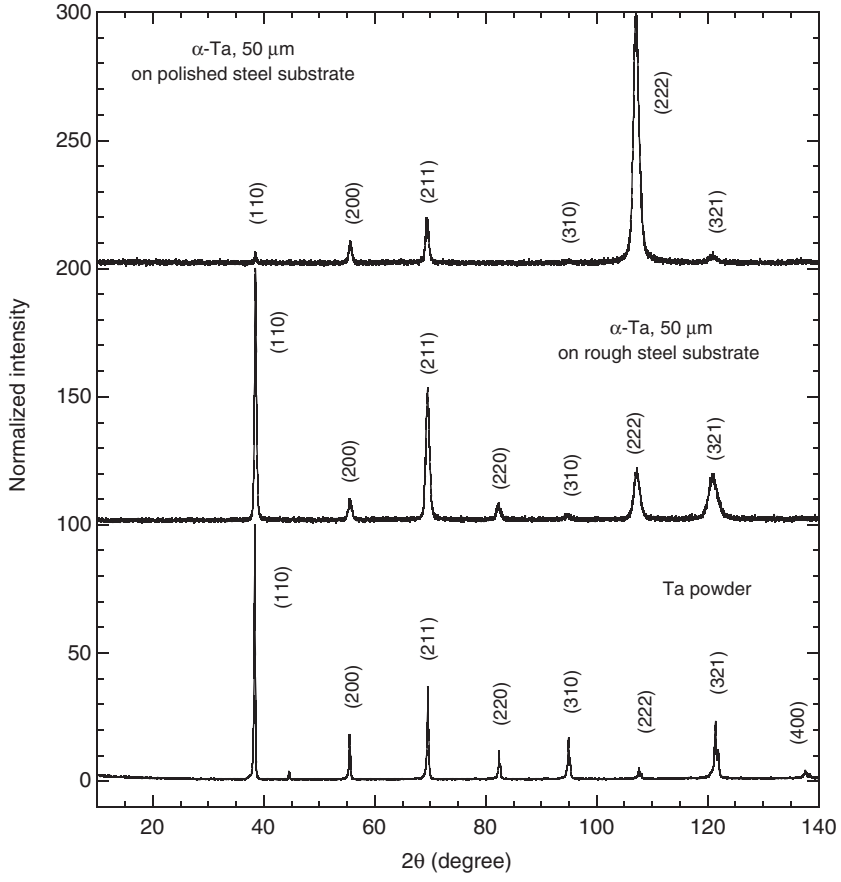

Fig. 1. X-ray diffraction patterns of α-Ta coatings on the smooth and rough steel substrates and Ta powder. XRD patterns are normalized with respect to the peak with maximum intensity in each spectrum.

selection, and the second Si crystal was detuned to approximately 80% of maximum transmitted X-ray intensity to minimize the presence of higher harmonics in the beam. Data from the coating and a reference Ta foil were collected over the energy range of 9.732–10.986 keV and analyzed following standard procedures [12].

The electrochemical corrosion behavior was studied with potentiodynamic polarization and electrochemical impedance spectroscopy (EIS) in deaerated 0.5 M H_2SO_4 using a Gamry PC4/300 potentiostat/galvanostat/ZRA system. Additional experimental details are described in an earlier study [5]. The working electrode (WE) was the coating with an exposure area of 1 cm^2 and a saturated calomel electrode (SCE) was employed as a reference electrode to measure the potential across the electrochemical interface. A platinum grid was used as the counter electrode (CE). Potentiodynamic polarization was measured at the corrosion potential (E_{corr}) 1 h after immersion in an effort to reach the quasi-stable potential. The polarization curves were obtained by sweeping from −0.2 to +1.5 V (vs. E_{corr}) with a scan rate of 10 mV/min. Impedance spectra in the frequency range from 10 mHz to 100 kHz, with an excitation signal amplitude of 10 mV (r.m.s.) at E_{corr}, and were collected over 0.5, 1, 4, 8, 24, 48, 72, and 96 h. The EIS data were interpreted on the basis of an equivalent circuit using complex nonlinear least squares fitting (CNLS) LEVM algorithm [13] in the Gamry Echem Analyst software.

3. Results and discussions

3.1. Phase and structure of the Ta coatings

The α-Ta coating on the polished steel substrate shows (222) preferred orientation, while the coating on the rough substrate exhibits a very similar pattern to Ta powder, in which (110) peak has the highest intensity (Fig. 1). All peaks can be indexed as α-Ta peaks. Peak broadening observed in all the peaks of both coatings, as compared to Ta powder, can be attributed to microstrain and particle size. In addition to the long range structure, the short range structure of both coatings was compared by conducting EXAFS. The Fourier transforms (FT) of the EXAFS ($\chi(k)k^3$) spectra (Fig. 2) over 1.78 to 3.05 Å correspond to the first coordination shell in the vicinity of the absorbing atom. This atomic short-range structure for both coatings is consistent with the theoretical EXAFS of α-Ta (Table 1) with 8–9 Ta atoms at 2.85 Å. It is interesting to note that only the long-range order is affected by the surface roughness while the short-range structure of the coatings on the two types of substrates appears to be the same.

The surface roughness of the substrates over 100 × 100 μm^2 area was measured by AFM to be 12.4 ± 1.9 nm (r.m.s.) for the smooth surface and 929.5 ± 246.1 nm (r.m.s.) for the rough surface (Fig. 3a and b). Subsequent to sputtering, the coating revealed the same order of magnitude in roughness with 62.6 ± 4.6 nm (r.m.s.) for the smooth substrate and 824.9 ± 80.6

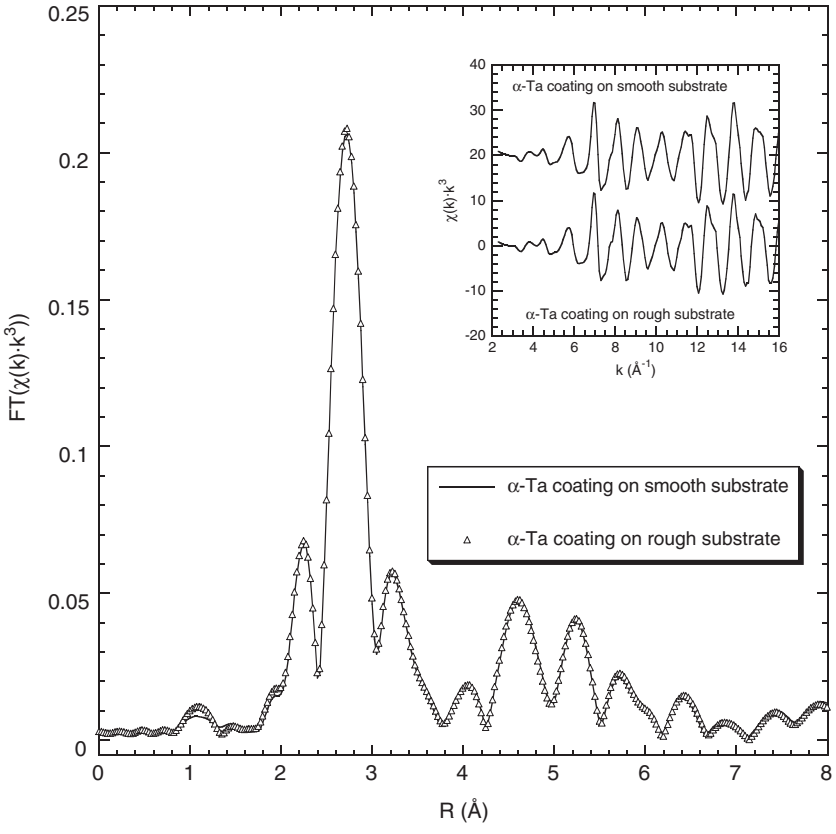

Fig. 2. Fourier transforms of Ta L_{III}–edge $\chi(k)k^3$ spectra of α-Ta coatings on the smooth and rough steel substrates over the k range 2.85–16.3 $Å^{-1}$. Ta L_{III}–edge $\chi(k)k^3$ spectra is shown in the insert.

Table 1
Results of EXAFS fits g^* on the first shell for α-Ta coating on the smooth and rough steel substrate Fourier transformed over 1.78 to 15.8 $Å^{-1}$ k-range and fitted over 1.78 to 3.05 Å r-range

	α-Ta coating on smooth steel substrate	α-Ta coating on rough steel substrate	α-Ta XRD model
N	8.81	8.60	8.00
R (Å)	2.85	2.85	2.86
σ^2($Å^2$)	0.005792±0.000064	0.005739±0.000120	0

N, R, and σ^2 are coordination number, interatomic distance, and Debye–Waller factor, respectively.
*S_0^2 was set as 1.0. N and R have errors of ±20% and ±0.02 Å, respectively.

nm (r.m.s.) for the rough one (Fig. 3c and d). These results indicate conformal coverage, with the film following the substrate topography (Fig. 3b and d). Interestingly, over 2×2 μm^2 scanned area (Fig. 3e and f), the roughness of Ta coatings on the smooth and rough substrates are 26.6±2.7 and 33.1±5.0 nm, respectively, indicating no significant difference in the microscopic roughness for the Ta coatings. Because of the limited vertical range of the AFM, the surface was also examined with a profilometer (Dektak) over 2 mm and showed an average roughness (Ra) of 1100.0±51.3 and 1054.5±129.7 nm, before and after deposition on the rough substrate. The peak to valley distance was approximately 5 μm. Furthermore, the FE-SEM images of the Ta coating on both types of substrates showed no apparent difference in their morphology (Fig. 4a and c). Droplet-like defects, which are commonly observed in the PVD films [14,15], are seen on the coated surface regardless of surface roughness (Fig. 4b and d). Although the AFM images at multiple scales suggest uniform coverage of both types of substrates, an analysis of open pores, or porosity, due to defects, is critical before concluding that the substrate roughness is not important for the coating viability.

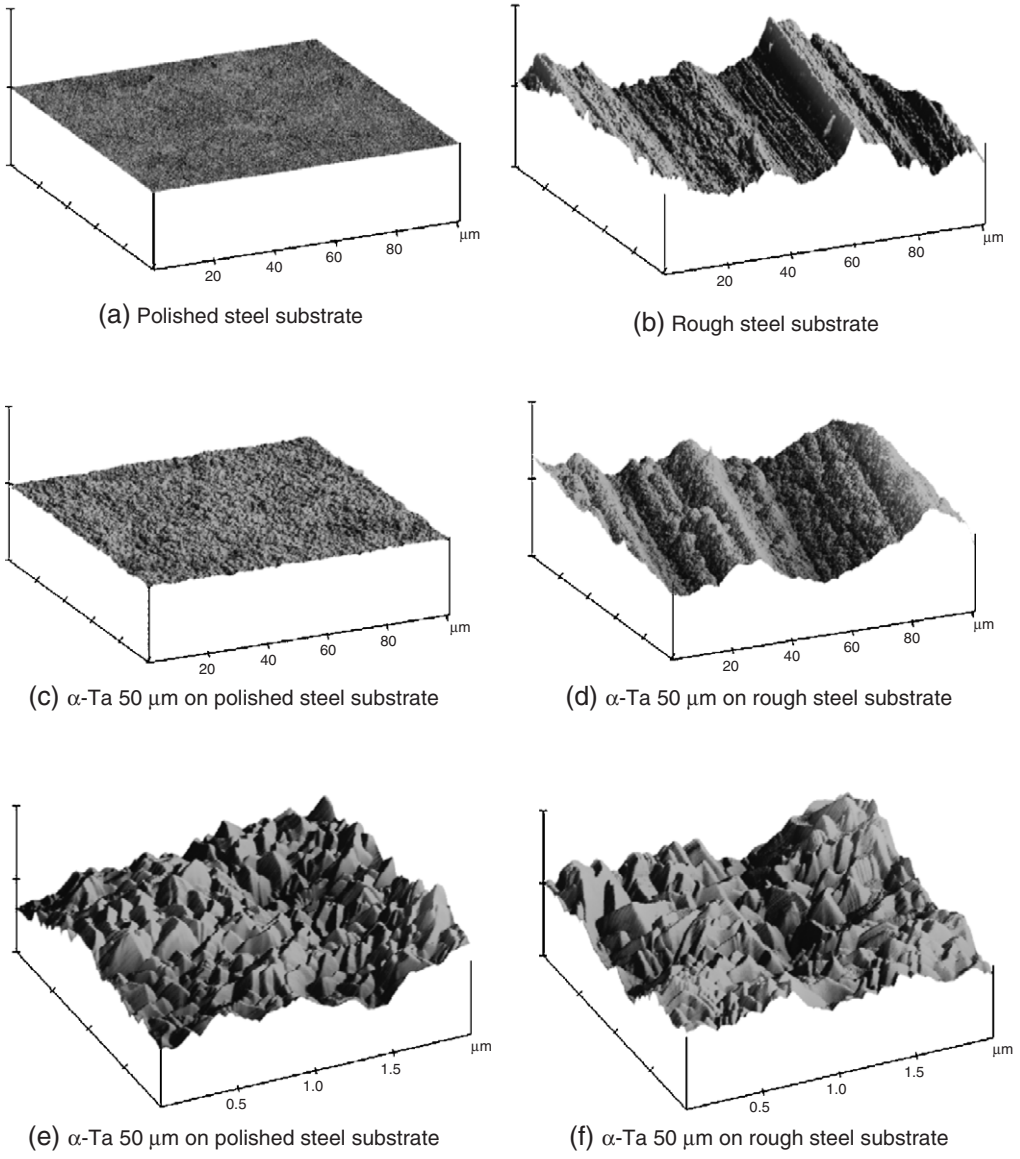

Fig. 3. AFM surface plots of the smooth and rough steel substrates (a, b) and α-Ta coatings on these substrates (c–f). Scans (a–d) were performed over 100×100 μm^2 area and scans (e–f) over 2×2 μm^2. The vertical z scale, unit is 5 μm for (a–d) and 200 nm for (e, f).

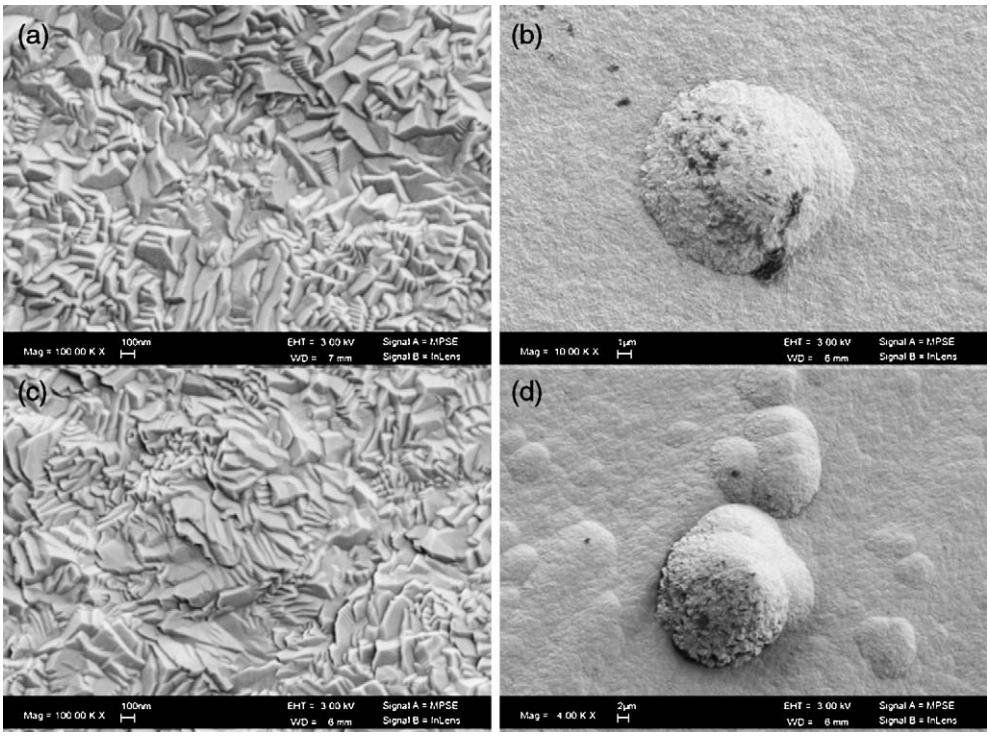

Fig. 4. SEM images of α-Ta coatings (50 μm thick) on the smooth and rough steel substrates showing droplet like defects; (a and b) α-Ta coating on smooth steel substrate and (c and d) β-Ta coating on rough steel substrate.

3.2. Porosity Assessment

Anodic polarization curves measured on smooth and rough steel substrates (AISI 4340), and the α-Ta coatings deposited on these substrates, in 0.5 M H_2SO_4 deaerated with N_2 at room temperature, are shown in Fig. 5. The results of measurements performed on a Ta foil are also shown for reference. Both the smooth and rough steel substrates show very similar polarization

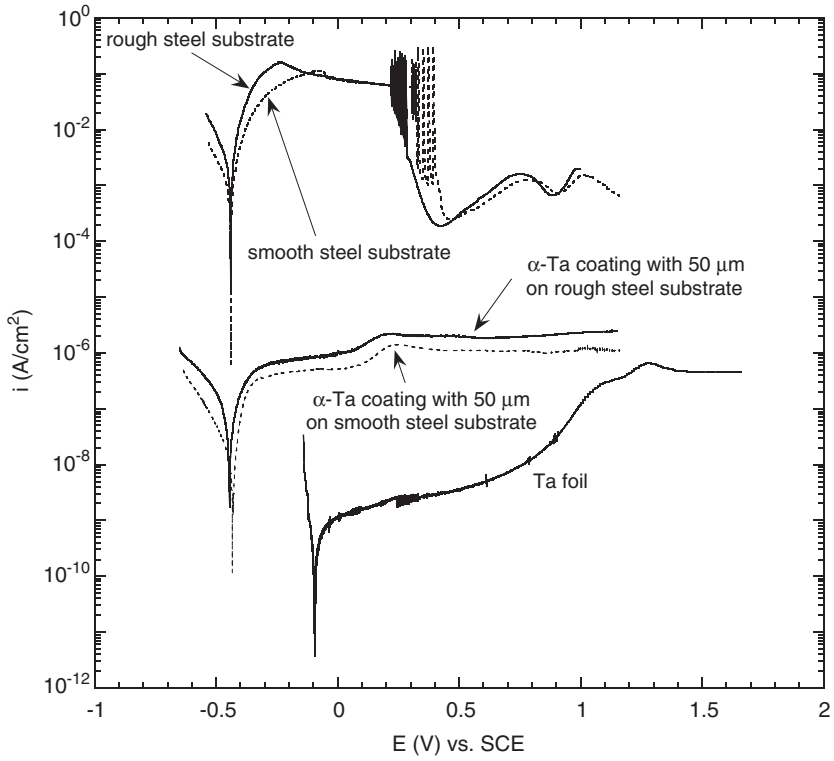

Fig. 5. Anodic polarization curves of smooth and rough steel substrates (AISI 4340), α-Ta coatings deposited on these substrates and of Ta foil, in 0.5 M H_2SO_4 deaerated with N_2 at room temperature.

Table 2
Electrochemical characteristics of α-Ta coating with different roughness, the smooth and rough steel substrate and Ta foil

	α-Ta coating with 50 μm thickness		Steel substrate		Ta foil
	On smooth substrate	On rough substrate	Smooth surface	Rough surface	
E_{corr} (mV vs. SCE)	−433	−445	−439	−440	−94
R_p (Ω)	1.09×10^6	2.97×10^5	13.54	5.20	3.14×10^7
b_a (mV/decade)			50.7	46.8	

behavior, except that the current density of the rough substrate before the passivation potential is greater than that of the smooth substrate (Fig. 5). The current density is based on 1 cm^2 of the exposed area. Therefore, considering that the actual surface area is proportional to surface roughness, the larger current density for the rough substrate may be attributed to a larger actual area as compared to the smooth substrate.

The α-Ta coatings on both substrates show almost identical polarization behavior regardless of surface roughness; however, the current density for the coating on the rough substrate is shifted upwards, which may be attributed to the roughness and coating porosity. Additionally, our previous study suggested no significant effect of crystallographic orientation on anodic polarization behavior of α-Ta [5]. Therefore, the difference in the current density over the passive region was not likely to be caused by the different orientation of the α-Ta coatings. At open circuit potential, the coatings exhibit approximately two orders of magnitude smaller polarization resistance than the Ta foil (Table 2). Nevertheless, the coating is chemically inert [5] and, hence, the polarization resistance at the open circuit potential represents the resistance of the steel substrate exposed to the electrolyte at the open pores. The porosity index, P, representing the area ratio of total pores to total exposed surface can be estimated using equation [6]:

$$P = \left(\frac{R_{ps}}{R_p}\right) \times 10^{-|\Delta E_{corr}|/b_a} \quad (1)$$

where R_p and R_{ps} are the polarization resistances of the Ta coated steel and bare steel substrate, respectively; ΔE_{corr} is the difference between the corrosion potentials of the Ta coating and the bare steel substrate; and b_a is the anodic Tafel slope for the bare steel substrate (Table 2). Eq. (1), with the measured polarization resistance data, gives the porosity of the coatings on the smooth and rough steel substrates as 7.92×10^{-4}% and 9.43×10^{-4}%, respectively, indicating a negligible difference. This result implies that the surface roughness of steel substrate does not significantly influence the quality of Ta coatings at 50 μm. However, the corrosion resistance may be impacted as a function of immersion time due to potential delamination of the

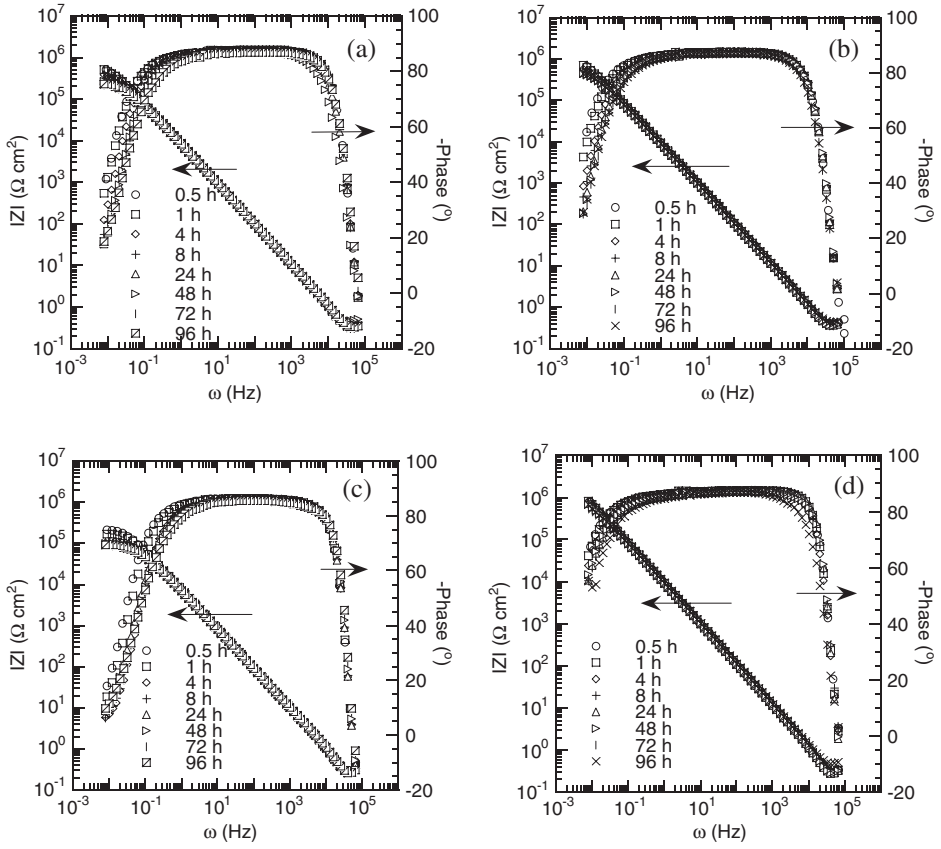

Fig. 6. Impedance spectra of α-Ta coatings for different immersion times in deaerated 0.5 M H_2SO_4 with N_2 at room temperature; (a) and (b) represent α-Ta coatings on smooth steel substrate; (c) and (d) β-Ta coatings on rough steel substrate.

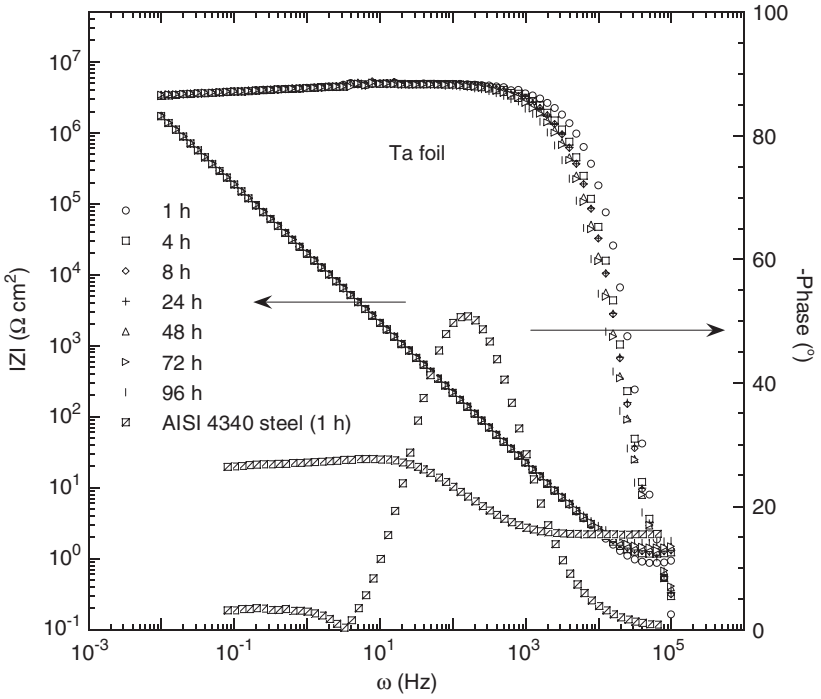

Fig. 7. Impedance spectra of Ta foil for different immersion times and of AISI 4340 steel for 1 h exposure time in deaerated 0.5 M H_2SO_4 with N_2 at room temperature.

coating initiated at open pores and/or blocking of open pores by corrosion product [14,16,17].

3.3. Corrosion behavior as a function of time

The results of the electrochemical impedance spectroscopy measurements are shown in Fig. 6. The spectra of α-Ta coatings on the smooth and rough steel substrates show that there is no significant change in the impedance at the lowest frequency over 4 days of exposure. The phase angle responses on these coatings are very similar to that measured on Ta foil, shown in Fig. 7. Only one relaxation time constant is present in the EIS spectra of the coatings and of Ta foil [4]. In the case of ceramic and polymer coatings, the magnitude of the impedance in low frequency range represents total resistance, which is sum of the polarization resistance of the metal substrate through open pores and the pore resistance [14–17]. Our previous EIS study demonstrated that as the degradation of the protective coating proceeds, a transformation from a single to two relaxation time constants was observed in the phase angle spectra [5]. However, substrate corrosion and coating delamination were not seen in that study.

The equivalent circuit (EC) model consisting of a parallel combination of a polarization resistance (R_p) and a constant phase element (CPE) in series with solution resistance (R_{sol}) was applied to fit the EIS data for Ta foil and the coatings (Fig. 8). For Ta foil, R_p represents the polarization resistance of the interface between Ta and electrolyte. As for the α-Ta coating, R_p characterizes the total resistance, which is the sum of the polarization resistance of the steel substrate through open pores and the resistance of the electrolyte in the pores of the Ta coating. The data presented in Fig. 9 show that R_p of Ta foil increases with the immersion time up to 4 h, and then remains constant for over 4 days. The increase in R_p may be due to passivation, which is confirmed by the increase in the corrosion potential as a function of immersion time. For the Ta coatings, R_{tot} decreases at initial times reflecting electrolyte penetration in the fine pores (Fig. 9) [16]. No further decrease in R_{tot} on either smooth or rough steel substrates is observed 8 h after immersion and in fact it becomes almost constant, as seen also with Ta foil. In addition, an EDX analysis showed no evidence of substrate corrosion through open pores. Therefore, the presence of open pores for such thick coatings is in question. Additionally, repeated depositions under the same sputtering conditions produced samples with the same values of R_{tot} regardless of the substrate roughness. This result demonstrates that there is no significant effect of substrate roughness on the coating quality for at least 50 ìm with respect to corrosion performance. Additionally, the small variation of total resistance (R_{tot}) for each sample indicated that the formation and distribution of pores were random.

Lee et al. [18] studied the corrosion behavior of 2.36 μm CrN films on steel substrate with roughnesses of 0.10, 0.20 and 0.31 μm (Ra), of which the ratio of coating thickness to substrate roughness was 23.6, 11.8, and 7.61, respectively.

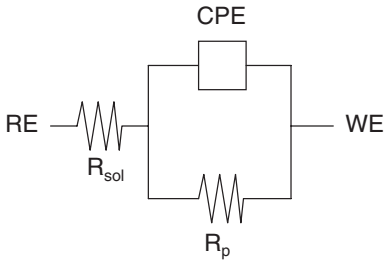

Fig. 8. Equivalent circuit models for fitting experimental EIS data of Ta foil and α-Ta coatings.

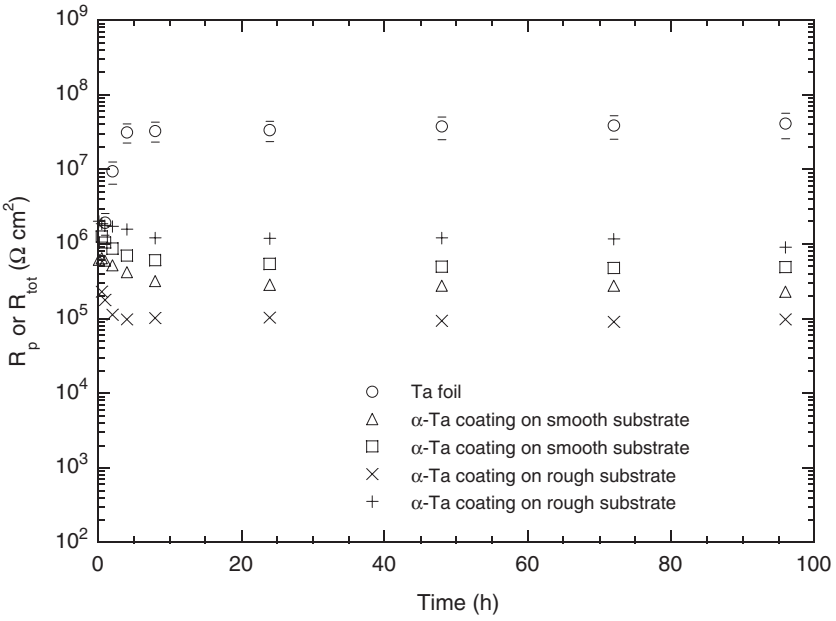

Fig. 9. R_p and R_{tot} of Ta foil and α-Ta coatings on the smooth and rough steel substrates as a function of time. Error bars not visible are present within symbol.

They observed that the coating porosity increased with increasing roughness and thus the corrosion rate increased. In all cases, coating failure was observed. Similarly, for a PVD CrN coating, Liu et al. [11] found a decrease in defects as surface roughness decreased with polishing, which changed from 220 grit SiC to a 6 μm diamond paste. Our results suggest the existence of a critical aspect ratio of the coating thickness to the substrate roughness, above which there is no effect of substrate roughness on the coating porosity.

4. Conclusions

The analysis of sputtered α-Ta coatings on steel showed that while the long-range crystallographic orientation, seen in XRD patterns, is affected by the substrate surface roughness, the short-range structure is equivalent to the bulk α-Ta. The latter has been demonstrated by EXAFS measurements of the Ta–Ta coordination in the first shell (1.78 Å $\leq R \leq$ 3.05 Å). Although the substrate surface roughness was two orders of magnitude greater for the coatings deposited on the rough substrate than the smooth one, the porosity was only 7.92×10^{-4}% for the smooth substrate and 9.43×10^{-4}% for the rough one, representing a negligible difference. The coatings deposited on both substrates showed almost identical anodic polarization behavior; although the corrosion current density was slightly higher in the case of the coating on the rough substrate. The potentiodynamic impedance behavior of the coatings over long exposure times was similar to that of Ta foil, revealing a high corrosion resistance. Moreover, repeated deposition under the same sputtering conditions on substrates with different roughness produced samples that had the same corrosion resistance over all exposure times studied. This result implies that there is no significant effect of substrate roughness on corrosion performance, at least when the ratio of coating thickness to the surface roughness (maximum surface height excursions) is greater than 10.

Acknowledgements

This work was conducted by NJIT as part of the Sustainable Green Manufacturing Program, through the National Defense Center for Environmental Excellence, contract DAAE30-98-C-1050.

References

[1] S.L. Lee, M. Cipollo, D. Windover, C. Rickard, Surf. Coat. Technol. 120–121 (1999) 44.
[2] S.L. Lee, D. Windover, M. Audino, D.W. Matson, E.D. McClanahan, Surf. Coat. Technol. 149 (2002) 62.
[3] L.A. Clevenger, A. Mutscheller, J.M.E. Harper, C. Cabral Jr., K. Barmak, J. Appl. Phys. 72 (1992) 4918.
[4] L. Gladczuk, A. Patel, C. Singh Puar, M. Sosnowski, Thin Solid Films 467 (2004) 150.
[5] S. Maeng, L. Axe, T.A. Tyson, L. Gladczuk, M. Sosnowski, Corr. Sci. (in press).
[6] B. Elsener, A. Rota, H. Bohni, Mat. Sci. Forum 44–45 (1989) 29.
[7] R. Brown, M.N. Alias, R. Fontana, Surf. Coat. Technol. 62 (1993) 467.
[8] J.L. He, C.H. Chu, H.L. Wang, M.H. Hon, Surf. Coat. Technol. 63 (1994) 15.
[9] H.A. Jehn, Surf. Coat. Technol. 125 (2000) 212.
[10] J. Munermasa, T. Kumakiri, Surf. Coat. Technol. 49 (1991) 496.
[11] C. Liu, A. Leyland, S. Lyon, A. Matthews, Surf. Coat. Technol. 76–77 (1995) 623.
[12] B.K. Teo, Extended X-ray Absorption Spectroscopy: Basic Principles and Data Analysis, Springer-Verlag, New York, 1986, p. 114.
[13] J.R. Macdonald, Impedance Spectroscopy, John Wiley and Sons Inc., New York, 1987, p. 173.
[14] C. Liu, Q. Bi, A. Leyland, A. Matthews, Corros. Sci. 45 (2003) 1257.
[15] S.H. Ahn, J.H. Lee, J.G. Kim, J.G. Han, Surf. Coat. Technol. 177–178 (2004) 638.
[16] D.K. Merl, P. Panjan, M. Cekada, M. Macek, Electrochim. Acta 49 (2004) 1527.
[17] F. Mansfeld, Electrochim. Acta 38 (1993) 1891.
[18] S Lee, W. Ho, F.D. Lai, Mater. Chem. Phys. 43 (1996) 266.